

NICST Internal Memo

Date: July 21, 2011
From: Jeff McIntire
To: Bruce Guenther, Jim Butler, and Jack Xiong
Subject: Solar Diffuser Stability Monitor Measurements from End-to-End Testing of the Reflective Solar Bands Using T-SIRCUS

References:

- [1] 'Facility for Spectral Irradiance and Radiance Responsivity Calibrations Using Uniform Sources,' S. W. Brown, G. P. Eppeldauer, and K. R. Lykke, Appl. Opt 45(32), 8218-8237 (2006).
- [2] NICST_MEMO_11_008, 'Solar Diffuser Stability Monitor Measurements from End-to-End Testing of the Reflective Solar Bands Using T-SIRCUS,' J. McIntire, July 6, 2011.
- [3] NICST_MEMO_08_043, 'VIIRS FU1 SD Prelaunch BRF for Both VIIRS and SDSM Views,' J. Sun and S. Xiong, December 17, 2008.
- [4] 'NIST Laser Collimator Non-Uniformity Corrections for VIIRS End-to-End Test,' J. McCarthy, April 6, 2010.
- [5] 'Performance Verification Report – VIIRS FU1 Reflective band Calibration (PVP Section 4.2.2),' B. Robinson, M. Bliton, R. Menzel, and D. Tyler, December 3, 2009.
- [6] *An Introduction to Error Analysis*, J. R. Taylor, University Science Books (1997).

1. Introduction

The End-to-End (E2E) test of the RSB calibration cycle was performed in March 2010 at the BATC facility in Boulder CO. The VIIRS F1 sensor had been integrated into the NPP spacecraft in January 2010. E2E testing utilized the NIST T-SIRCUS as a source [1].

This memo will describe the analysis of the E2E measurement of the SDSM calibration cycle (the SD measurements were discussed in a separate memo [2]). Table 1 lists the data used in this work.

2. Analysis Methodology

2.1 Test Description

T-SIRCUS consists of a series of tunable lasers; for E2E testing, a Ti:sapphire laser was used in continuous wave mode to produce monochromatic illumination at 742 and 852 nm (and frequency doubling was used to reach 442 nm) [1].

The T-SIRCUS was used to feed two sources via fiber optics: an integrating sphere and a collimator (only the collimator is used for SDSM testing). The collimator was positioned to illuminate both the SD view and the SDSM solar view simultaneously. The exit aperture of the collimator was about 25 inches in diameter. A total of seven collimator positions were performed covering five different angles, listed in Table 1 in the order performed. Note that the first, fourth, and fifth positions are repeated measurements of roughly the same angle. An irradiance monitor was positioned near the center of the collimator exit aperture, from which real-time tracking of the irradiance was performed. Pre-determined calibration coefficients were used to convert the monitor output from volts to irradiance.

VIIRS data for E2E testing was recorded in a three data collect cycle. During the first collect in each cycle, the SDSM mirror was rotating and data was recorded. Each of these collects contained 128 VIIRS scans (roughly 3.8 minutes) in diagnostic mode. For most collimator positions, this cycle was conducted twice per measured wavelength (except position 5 when it was conducted only once). Data collects were recorded with the SIRCUS output at 442, 742, and 852 nm (442 nm was only measured once during collimator position 7); this corresponds to VIIRS SDSM detectors 2, 6, and 7 (see Table 1).

2.2 SDSM Ratio Determination

The measured SDSM ratio is defined as follows:

$$R_{measured} = \frac{(DN_{SD} - DN_{dark})}{(DN_{solar} - DN_{dark})}. \quad (1)$$

The $R_{measured}$ is determined every three scans and is trended over a particular calibration cycle as well as across calibration cycles. This allows for tracking of the temporal changes in the SD BRF.

The radiance reaching a SDSM detector using the SD path is

$$L_{SD} = \frac{\gamma_2 E_{mon}}{\Omega_{sun}} \tau_{SAS} \frac{BRF_{SDSM}}{\pi} \cos \theta_{SD} \pi \sin^2 \psi, \quad (2)$$

where

$$\tau_{SAS} = 0.1258(1 - 0.1538 \tan \delta)(1 - 0.04746 \tan \phi) \quad (3)$$

Here ϕ and δ are the azimuthal and declination angles in spacecraft coordinates. The $\cos \theta_{SD}$ is the projection of the incident irradiance on the SD; it is defined as the dot product of the SD normal vector (0.29724, -0.21860, 0.92944) and the sun vector [5]

$$\vec{n}_{sun} = \frac{1}{\sqrt{1 + \tan^2 \phi + \tan^2 \delta}} (1, -\tan \phi, \tan \delta). \quad (4)$$

The BRF was fit to a quadratic polynomial in both declination and azimuthal angles [3], or

$$BRF_{SDSM} = c_0 + c_1 \delta + c_2 \phi + c_3 \delta^2 + c_4 \phi^2 + c_5 \delta \phi, \quad (5)$$

where the coefficients were determined at wavelengths 400, 500, 600, 700, and 900 nm. The BRF used here is interpolated between the two nearest wavelengths. E_{mon} is the

collimator monitor irradiance and γ_2 is the collimator uniformity correction (as yet undetermined [4]). The solid angle subtended by the sun as seen from VIIRS is given by Ω_{sun} . The factor of $\pi \sin^2 \psi$ corresponds to the solid angle of the entrance cone on the SDSM for the SD view, where the half angle of the cone, ψ , is 7.78 degrees.

The radiance illuminating a SDSM detector using the solar path is

$$L_{SD} = \frac{\gamma_3 E_{mon}}{\Omega_{sun}} \tau_{SDSM} . \quad (6)$$

τ_{SDSM} is the transmission factor for the SDSM screen. This transmission includes the cosine of the projection angle onto the SDSM screen. In addition, because the detectors are located inside the SDSM integrating sphere, each detector has a direct view of the reflection of the image on the inside of the sphere. This results in each detector observing a slightly different radiance based on its location inside the integrating sphere [5]. Note that the collimator uniformity correction (γ_2) for the SDSM SD view is different from the correction for the solar view of the SDSM (γ_3); both corrections are as yet undetermined [4].

The theoretical SDSM ratio is the ratio of Eqs. (2) and (6), or

$$R_{calculated} = \frac{\gamma_2}{\gamma_3} \frac{\tau_{SAS}}{\tau_{SDSM}} \cos \theta_{SD} BRF_{SDSM} \sin^2 \psi . \quad (7)$$

The source radiance cancels (excepting the uniformity corrections) and what remains is the ratio of the transmission factors in each optical path.

2.3 Uncertainty Analysis

The error in the calculated SDSM ratio is defined by the standard error propagation [6]

$$\frac{u^2(R_{calculated})}{R_{calculated}^2} = \frac{u^2(\tau_{SAS})}{\tau_{SAS}^2} + \frac{u^2(\tau_{SDSM})}{\tau_{SDSM}^2} + \frac{u^2(\cos \theta_{SD})}{\cos^2 \theta_{SD}} + \frac{u^2(BRF_{SDSM})}{BRF_{SDSM}^2} + 4 \frac{u^2(\sin \psi)}{\sin^2 \psi} + \frac{u^2(\gamma_2)}{\gamma_2^2} + \frac{u^2(\gamma_3)}{\gamma_3^2} . \quad (8)$$

Since all of these factors in $R_{calculated}$ were measured independently, it is assumed that there are no correlations between the uncertainties of the various factors.

Due to the large variability in the SDSM measurement over any given data collection (as shown in Figures 1 and 2), the error on the average SDSM ratio per data collection is taken to be the standard deviation of all individual SDSM ratios within that data collection.

The error in the SAS transmission, the SDSM screen transmission, and the SDSM BRF were determined by the sensor subcontractor [5], and are 0.24 %, 0.67 %, and 1.09 %, respectively. The uncertainty in the cosine of the projection angle is determined from alignment measurements made using theodolites. The measurements are assumed to be known to 0.01 degrees. That uncertainty is propagated through to the cosine of the projection angle. The SDSM entrance cone angle is also assumed to be known to 0.01

degrees; the uncertainty is propagated to the solid angle of the entrance cone. The determination of the uncertainties for the collimator uniformity correction factors is in progress; for the purposes of this work, they are not included in the final results presented below. The final calculated SDSM ratio uncertainties are defined by Eq. (8) for each data collection.

3. Analysis Results

3.1 Data Quality and Reduction

Five SDSM pixels were recorded every scan for each detector in the SDSM integrating sphere. These five pixels were averaged for every scan. The averaged DN from each three scan cycle was used to determine the ratio in Eq. (1). This SDSM ratio was trended versus time for each data collection and collimator angle. In addition, the average of the ratios for each data collection was determined. As the SDSM was illuminated with monochromatic light, only the detector corresponding to the input wavelength was analyzed. As with the SD data, some data collections were missing scans; again, the data was retained for those scans that appeared to be valid data. The collimator uniformity corrections (γ_2 and γ_3) were not applied in this work.

3.2 SDSM Ratio Results

The measured SDSM ratios [as defined by Eq. (1)] are plotted in Figures 1 and 2. Each color represents a different collimator position (solid and dashed lines indicating first and second data collections at a particular collimator position). The ratios are between 1.1 and 1.3 for 742 nm and between 1.15 and 1.35 for 852 nm. In addition, the measured ratios exhibited one sigma variation of up to 2.7 % over roughly 3.8 minutes (the temporal fluctuations in the solar view is generally larger than in the SD view). On MODIS, the SDSM also exhibits large variation in any given detector over a typical solar observation; fortunately, all the SDSM detectors vary in roughly the same manner. This allows the temporal variation to be removed using the response of MODIS SDSM detector 9 (936 nm). Due to the fact that T-SIRCUS was a narrow band source, only one SDSM detector recorded a meaningful signal for a particular data collection; as a result, the temporal trend could not be removed in this test using the MODIS methodology.

The measured ratios, averaged over each data collection, are plotted versus collimator position number in Figures 3 and 4 for 742 nm and 852 nm, respectively. Black crosses and red asterisks indicate the first or second data collections at a particular collimator position (where the error bars are \pm one standard deviation over that data collection). The measured SDSM uncertainties as defined above were between roughly 0.5 and 2.7 %. The blue diamonds represent the calculated ratio at each collimator position. The calculated error was approximately 1.38 % (this number was fairly constant as the major factors were not wavelength or angle dependent). The largest contributors were the SD BRF (1.09 %) and τ_{SDSM} (0.67 %). The measurements were consistent with the theoretical values for all positions at 742 nm (with the exception of position 3, measurement 1).

However, most measurements were not consistent with the theoretical results at 852 nm (and sometimes also inconsistent between measurements 1 and 2).

4. Summary

- E2E testing was an exploratory use of tunable lasers applied to the characterization of the reflective band calibration cycle. Results are preliminary (collimator uniformity corrections as yet undetermined).
- Measured SDSM ratios consistent with theoretical estimates at 742 nm, but largely inconsistent at 852 nm. The largest contributors to the theoretical uncertainty are the SD BRF and τ_{SDSM} .
- Large short-term variability in SDSM ratios. Narrow band source prevents removal of temporal variability using 935 nm detector (as done on MODIS).

Acknowledgement

The sensor test data used in this document was provided by the BATC testing team. Approaches for data acquisition and data reductions, as well as data extraction tools were also provided by the Raytheon El Segundo team. We would like to thank the Raytheon El Segundo and BATC teams for their support. The data analysis tools were developed by the NICST team.

Table 1: E2E SDSM test data

Collimator Position	Date	Declination δ	Azimuthal φ	Wavelengths (SDSM detector)	UAIDs	Collects
1	March 19, 2010	22.52	16.31	742 (6); 852 (7)	4742; 4744	1, 4; 1, 4
2	March 19, 2010	13.64	16.87	742 (6); 852 (7)	4746; 4747	1, 4; 1, 4
3	March 19, 2010	30.09	16.34	742 (6); 852 (7)	4749; 4750	1, 4; 1, 4
4	March 19, 2010	22.37	16.44	742 (6); 852 (7)	4751; 4752	1, 4; 1, 4
5	March 20, 2010	22.38	16.52	742 (6); 852 (7)	4753; 4754	1; 1
6	March 20, 2010	30.44	15.21	742 (6); 852 (7)	4755; 4756	1, 4; 1, 4
7	March 20, 2010	13.63	15.07	442 (2); 742 (6); 852 (7)	4758; 4759; 4760	1, 4; 1, 4; 1, 4

Figure 1: SDSM ratios for 742 nm (SDSM detector 6)

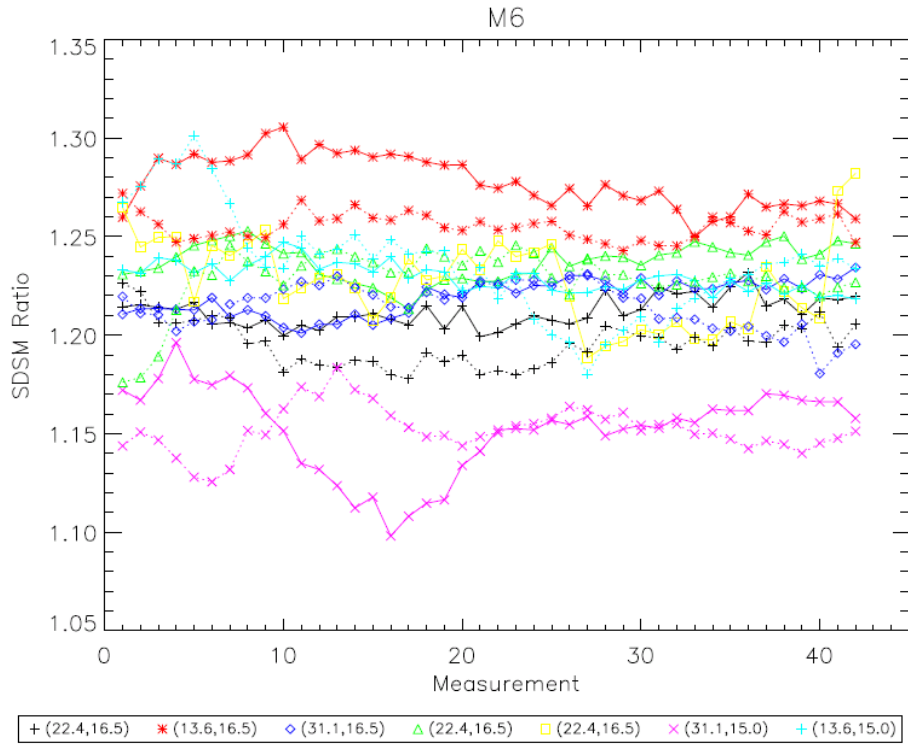


Figure 2: SDSM ratios for 852 nm (SDSM detector 7)

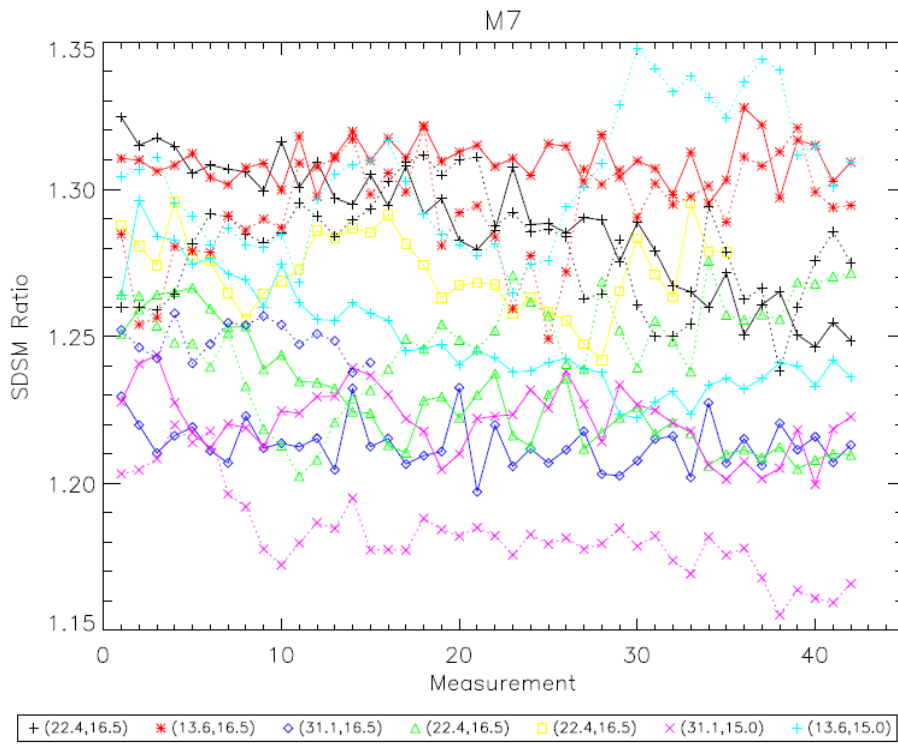


Figure 3: Averaged SDSM ratios with uncertainties (SDSM detector 6)

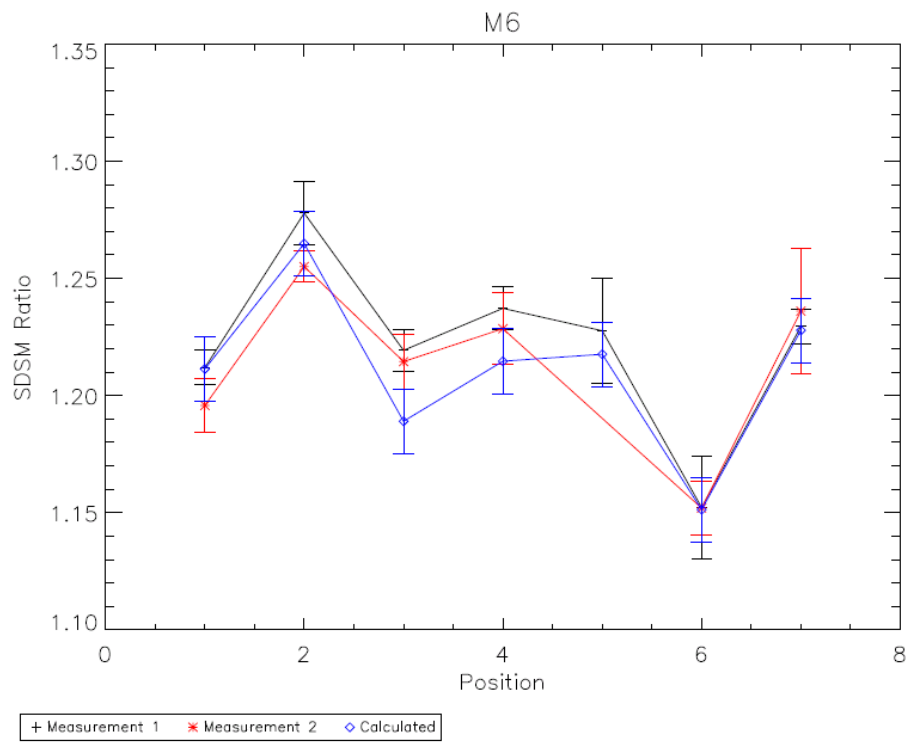


Figure 4: Averaged SDSM ratios with uncertainties (SDSM detector 7)

